LINEAR PHASE VELOCITY EFFECT ON ACCUMULATION OF ZINC IN HOMOGENEOUS FINE SAND APPLYING PREDICTIVE MODEL

Ezeilo. F.E [1], Eluozo. S. N [2]
[1]Department of Civil Engineering
Rivers State University of Science and Technology Port Harcourt.
E-mail: ezeilo.ebele@ust.edu.ng
Gregory University Uturu (GUU)
Abia State of Nigeria
[2]Department of Civil Engineering,
E-mail: Soloeluozo2013@hotmail.com

Abstract

The behaviour of velocity in predominant sand gravel was observed to affect the accumulation of zinc in sand gravel deposition; the concept of this study was to monitor the rate of zinc deposition pressured by linear fluids velocity deposition in sand gravel formation. Base on these factors, zinc deposition in sand gravel through velocity of flow pressure experiences slight fluctuations in some deposited depths of the formations; these are observed where linear velocity of flow was found predominant. The effect on zinc deposition also observed variations of velocities base on the stratification as it is expressed on the lithology. The formations in some locations experiences low velocities thus zinc concentration where very high in these few simulated results. The developed model generated theoretical values. Simulation results show that zinc concentration varies from 1.12 to 10.4 mg/l , 8.49E-05 mg/l to1.19E-03mg/l and 4.77E-03mg/l to 6.32 E-03mg/s at depths of 3-30metres and 3-36metres respectively. These data were compared with experimental values and both parameters compared favourably well. Experts in soil and water engineering will definitely use this concept as a tool in design of environmental systems.

Keywords: mathematical model, plug flow, linear velocity and homogeneous sand gravel

Introduction

Most designs of deep geological repository for high level radioactive wastes (HLW) are based on the multi-barrier concept with isolation of the waste from the environment. The multi-barrier concept includes the natural geological barrier (host rock), engineered barriers made up of compacted sand-Bentonite mixtures (placed around waste containers or used as buffer and sealing elements) and metal canister. Compacted Bentonite-based materials are relevant materials for this purpose thanks to their low permeability, high swelling and high radionuclide retardation capacities (Pusch, 1979; Yong et al., 1986; Villar and Lloret, 2008; Komine and Watanabe, 2010; Cui et al., 2011). Engineered barriers are often made up of compacted bricks. When bricks are placed around waste canisters or to form sealing buffers, the so-called

technological voids either between the bricks themselves or between bricks, canisters and the host rock are unavoidable. As an example, 10 mm thick gaps between Bentonite blocks and canister and 25 thick mm gaps between the Bentonite blocks and the host rock have been considered in the basic design of Finland (Juvankoski, 2010). These technological voids appeared to be equal to 6.6 % of the volume of the gallery in the FEBEX mock-up test (Martin et al., 2006). Once placed in the galleries, engineered barriers are progressively hydrated by pore water infiltrating from the host-rock. This water infiltration is strongly dependent on the initial state of the compacted material (water content, suction and density, e.g. Cui et al. 2008). Indeed, it has been shown that water transfer in unsaturated swelling compacted Bentonite or sand Bentonite mixtures is strongly dependent on the imposed boundary conditions in terms of volume change. As shown in Yahia-Aissa et al. (2001), Cui et al. (2008) and Ye et al. (2009), the degree of swelling allowed significantly affects the amount of infiltrated water, with much water absorbed when swelling is allowed and a minimum amount of water absorbed when swelling is prevented. Volume change conditions also appeared to have, through microstructure changes, significant influence on the hydraulic conductivity. In this regard, the degree of swelling allowed by the technological voids described above has a significant influence on the hydro-mechanical behaviour of the compacted Bentonite and their effects need to be better understood. Swelling results in a decrease in dry density that may lead to a degradation of the hydro-mechanical performance of engineered barriers (Komine et al., 2009, Komine, 2010). As a result, the safety function expected in the design may no longer be properly ensured. Therefore, a better understanding of the effects of the technological voids is essential in assessing the overall performance of the repository.

3. Developed Governing Equation

$$\bar{V}\frac{\partial c}{\partial t} = \frac{\phi}{ne}\frac{\partial c}{\partial z} - Kx\frac{\partial c}{\partial z} \qquad \ldots\ldots\ldots\ldots\ldots\ldots \qquad (1)$$

Nomenclature

q = Aquifer height [L]

$\bar{V}$ = Homogeneous velocity [LT^{-1}]

K_x = Permeability coefficient [LT^{-1}]

ϕ = Flow rate [LT^{-1}]

ne = Porosity [-]

T = Time [T]

Z = Depth [L]

$$\frac{\partial c}{\partial t} = S^1C(t) - C(o) \quad \ldots\ldots\ldots\ldots\ldots\ldots \quad (2)$$

$$\frac{\partial c}{\partial z} = S^1C(z) - C(o) \quad \ldots\ldots\ldots\ldots\ldots\ldots \quad (3)$$

$$\frac{\partial c}{\partial z} = S^1C(z) - C(o) \quad \ldots\ldots\ldots\ldots\ldots\ldots \quad (4)$$

Substituting equation (2), (3) and (4) into equation (1) yields:

$$S^1C(t) - \bar{V}\left[\bar{V}S^1C(t) - C(o)\right] + \frac{\phi}{ne} + Kx\left[S^1C(x) - C(o)\right] \quad \ldots\ldots\ldots \quad (5)$$

$$S^1C(t) - \bar{V}\left[\bar{V}\,S^1C(t) - \frac{\phi}{ne}SC(x) + KxS^1C(x)\right] \quad \ldots\ldots\ldots\ldots \quad (6)$$

$$C(t) = {}^{1}\!/_{S}\left[\bar{V}S^1\,C(t) - \frac{\phi}{ne}S^1\,C(x) + KxS^1C(x)\right] \quad \ldots\ldots\ldots\ldots \quad (7)$$

$$C(t) = {}^{1}\!/_{S^1}\left[\bar{V}\,S^1C(t) - \frac{\phi}{ne}S^1\,C(x) + KxC(x)\right] \quad \ldots\ldots\ldots\ldots \quad (8)$$

$$C(t) = \frac{\bar{V} - \frac{\phi}{ne} + Kx}{S^1} \quad \ldots\ldots\ldots\ldots \quad (9)$$

$$\boxed{C(t) = C(t) - \bar{V} + \frac{\phi}{ne}V + Kx} \quad \ldots\ldots\ldots\ldots \quad (10)$$

$$C(t) = S^1C(t) = \bar{V}\;C(t) + \frac{\phi}{ne} + KxC^1 \quad \ldots\ldots\ldots\ldots \quad (11)$$

$$C(o) = \left[\bar{V}\,C(t) + \frac{\phi}{ne} + Kx\right]C(t) \qquad \ldots\ldots\ldots\ldots\ldots \qquad (12)$$

$$S^1C(t) = \left[\bar{V} - \frac{\phi}{ne} + Kx\right]C(t) \qquad \ldots\ldots\ldots\ldots\ldots \qquad (13)$$

$$C(t) = \frac{S^1C(t)}{\bar{V} + \frac{\phi}{ne} + Kx} \qquad \ldots\ldots\ldots\ldots\ldots \qquad (14)$$

$$C(t) = \frac{S^1(t)}{\bar{V} + \frac{\phi}{ne} + Kx} \qquad \ldots\ldots\ldots\ldots\ldots \qquad (15)$$

Furthermore, considering the boundary condition, we have at

$$t = 0 \;\; C^1(o) = C(o) = 0$$

$$C(t) = \left[\bar{V}\,S^1\;C(t) - \frac{\phi}{ne}C(x) + Kx\;C(x)\right] = 0 \qquad \ldots\ldots\ldots\ldots\ldots \qquad (16)$$

$$\frac{0}{\bar{V} - \frac{\phi}{ne} - Kx} = 0 \qquad \ldots\ldots\ldots\ldots\ldots \qquad (17)$$

Considering the following boundary condition in the equation

$$C(t) - Co - \bar{V}S^1\;C(t) - \bar{V}Co - S^1(t) + \frac{\phi}{ne}C(x) + \frac{\phi}{ne}Co\;S^1C(x)$$

$$+ KxS^1(x) + KxCo + S^1(x) \qquad \ldots\ldots\ldots\ldots\ldots\ldots\ldots \qquad (18)$$

$$C(t) = \bar{V}\,C(t) = SC(t)\;Co - \bar{V} + \frac{\phi}{ne} + KxCo \qquad \ldots\ldots\ldots\ldots\ldots \qquad (19)$$

Considering the denominator in the equation, we have

$$C(t) = \left[\bar{V} + \frac{\phi}{ne} + Kx\right]Co \qquad \ldots\ldots\ldots\ldots\ldots \qquad (20)$$

Considering $\frac{\phi}{ne} = \frac{1}{\bar{V}}$

$$C(t) = \left|\frac{1}{\bar{V}} + \bar{V} + Kx\right|Co \qquad \ldots\ldots\ldots\ldots\ldots \qquad (21)$$

$$C(t) = \left|\frac{1+V^2 + VKx}{\bar{V}}\right|Co \qquad \ldots\ldots\ldots\ldots\ldots \qquad (22)$$

$$C(t) = \left|\left(1+V^2 + VKx\right)\frac{1}{V}\right|Co \qquad \ldots\ldots\ldots\ldots\ldots \qquad (23)$$

$$C(t) = \left|\left(1+V^2 + VK\right)\frac{\phi}{ne}\right|Co \qquad \ldots\ldots\ldots\ldots\ldots \qquad (24)$$

$$C(t) = \lambda \qquad \ldots\ldots\ldots\ldots\ldots \qquad (25)$$

$$\lambda = \left|\left(1+V^2 + VK\right)\frac{\phi}{ne}\right|Co \qquad \ldots\ldots\ldots\ldots\ldots \qquad (26)$$

$$\lambda = \left|\frac{\phi}{ne} + \frac{\phi}{ne}V^2 + \frac{\phi}{ne}VKx\right|Co \qquad \ldots\ldots\ldots\ldots\ldots \qquad (27)$$

$$\frac{\phi}{ne}V^2 + \frac{\phi}{ne}KxV_{Co} + \left[\frac{\phi}{ne}Co - \lambda\right] = 0 \qquad \ldots\ldots\ldots\ldots\ldots \qquad (28)$$

Applying quadratic expression to equation (28), we have

$$V^2 + \frac{\phi}{ne}Kx + \left[\frac{\phi}{ne} - \lambda\right] = 0$$

Where a = $\frac{\phi}{ne}V^2$, b = $\frac{\phi}{ne}KxVCo$ and c = $\frac{\phi}{ne}\lambda$

$$V = \frac{-b \pm \sqrt{b^2 - 4ac}}{2a} \quad \ldots\ldots\ldots\ldots\ldots \quad (29)$$

$$V = \frac{-\frac{\phi}{ne} KxVCo \sqrt{\frac{\phi}{ne} KxVCo^2 - 4 \frac{\phi}{ne} V \frac{\phi}{ne} \lambda}}{2\frac{\phi}{ne} V} \quad \ldots\ldots\ldots\ldots\ldots \quad (30)$$

$$V_1 = \frac{-\frac{\phi}{ne} KxVCo + \sqrt{\frac{\phi}{ne} KxVCo^2 - 4 \frac{\phi}{ne} V \frac{\phi}{ne} \lambda}}{2\frac{\phi}{ne} V} \quad \ldots\ldots\ldots\ldots\ldots \quad (31)$$

$$\phi\Lambda_2 = \frac{-\frac{\phi}{ne} KxVCo - \sqrt{\frac{\phi}{ne} KxV\,Co^2 - 4\frac{\phi}{ne} V \frac{\phi}{ne} \lambda}}{2\frac{\phi}{ne} V} \quad \ldots\ldots\ldots\ldots\ldots \quad (32)$$

Since we have $A\ell^{st} + B\ell^{st}$, it implies that

$$qt = A\exp \frac{\frac{\phi}{ne} KxVCo + \sqrt{\frac{\phi}{ne} KxVCo^2 - 4 \frac{\phi}{ne} V \frac{\phi}{ne} \lambda}}{2\frac{\phi}{ne} V} \quad \ldots\ldots\ldots\ldots\ldots \quad (33)$$

If A = B = 1

$$q(t) = \exp\left[- \frac{\frac{\phi}{ne} KxVCo + \sqrt{\frac{\phi}{ne} KxVCo^2 - 4 \frac{\phi}{ne} V \frac{\phi}{ne} \lambda}}{2\frac{\phi}{ne} V} t \right] + \ell^{\left[- \frac{\frac{\phi}{ne} KxV\,Co + \sqrt{\frac{\phi}{ne} KxV\,Co^2 + 4 \frac{\phi}{ne} V \frac{\phi}{ne} \lambda}}{2\frac{\phi}{ne} V} \right] t} \quad (34)$$

Applying inverse Laplace of the equation yield

$$q(t) = \left[t + \frac{\phi}{ne} KxVCo \right] Co \left[- \frac{\frac{\phi}{ne} KxVCo + \sqrt{\frac{\phi}{ne} KxVCo^2 + 4 \frac{\phi}{ne} V \frac{\phi}{ne} \lambda}}{2\frac{\phi}{ne} V} t \right]$$

$$\left[\left[-\frac{\frac{\phi}{ne}KxVCo\sqrt{\frac{\phi}{ne}KxVCo^2+4}\frac{\phi}{ne}V\frac{\phi}{ne}\lambda}{2\frac{\phi}{ne}V}\right]\right]t-\left[\frac{\frac{\phi}{ne}KxVCo-\sqrt{\frac{\phi}{ne}KxVCo^2+4}\frac{\phi}{ne}V\frac{\phi}{ne}\lambda}{2\frac{\phi}{ne}V}\right]t \quad (35)$$

$$qt=\left[\frac{\phi}{ne}KxVCo\Big/t^2\ Co\right]\left[-\frac{\frac{\phi}{ne}KxVCo+\sqrt{\frac{\phi}{ne}KxVCo^2-4}\frac{\phi}{ne}V\frac{\phi}{ne}\lambda}{2\frac{\phi}{ne}V\phi\Lambda}\right]$$

$$\left[\left[-\frac{\frac{\phi}{ne}VKxCo\sqrt{\frac{\phi}{ne}KxVCo^2-4\frac{\phi}{ne}}V\frac{\phi}{ne}\lambda}{2\frac{\phi}{ne}V}\right]\right]\ell^{\left[-\frac{\frac{\phi}{ne}KxVCo\sqrt{\frac{\phi}{ne}KxVCo^2-4}\frac{\phi}{ne}V\frac{\phi}{ne}\lambda\phi\Lambda V\beta}{2\frac{\phi}{ne}V}\right]t}$$

$$-\left[-\frac{\frac{\phi}{ne}KxVCo\sqrt{\frac{\phi}{ne}KxVCo^2-4}\frac{\phi}{ne}V\frac{\phi}{ne}\lambda}{2\frac{\phi}{ne}V}\right]t \quad (36)$$

At this point $Co=\phi t\ \neq 0$

for equation (34) at $t=0\ C(o)=Co$, we have

$$Co=\left[\frac{\phi}{ne}KxVCo+\frac{\phi}{ne}V+\frac{\phi}{ne}x\right]Co\ [1+1+1]=0$$

$$=\left[\frac{\phi}{ne}KxVCo+\frac{\phi}{ne}V+\frac{\phi}{ne}\lambda\right]$$

Hence $\frac{\phi}{ne}KxV+\frac{\phi}{ne}V+\frac{\phi}{ne}\lambda=0$

Equation (37) can be written as:

$$qx = Co\ [t+2]\left[-\frac{\frac{\phi}{ne}KxVCo+\sqrt{\frac{\phi}{ne}KxVCo^2-4\frac{\phi}{ne}V\frac{\phi}{ne}\lambda}}{2\frac{\phi}{ne}V}\right]t$$

$$\left[\frac{\frac{\phi}{ne}KxVCo\sqrt{\frac{\phi}{ne}KxVCo^2-4\frac{\phi}{ne}V\frac{\phi}{ne}\lambda}}{2\frac{\phi}{ne}V}\right]t \qquad (37)$$

If $t = \frac{d}{v}$

$$C(z) = Co\left[\frac{d}{v}+2\right]\left[\frac{\frac{\phi}{ne}KxVCo\sqrt{\frac{\phi}{ne}KxVCo^2-4\frac{\phi}{ne}V\frac{\phi}{ne}\lambda}}{2V\phi\Lambda}\right]\frac{d}{v}$$

$$\left[\frac{\frac{\phi}{ne}KxVCo\sqrt{\frac{\phi}{ne}KxVCo^2-4\frac{\phi}{ne}V\frac{\phi}{ne}\lambda}}{2V\phi\Lambda}\right]\frac{d}{v} \qquad (38)$$

3. **Materials and method**

Standard laboratory experiment where performed to monitor the rate of zinc deposition at different formation, the soil deposition of the strata were collected in sequences base on the structural deposition at different study area, this samples collected at different location generate variation at different depth producing different migration of zinc concentration through its pressure flow at the lower end of the column at different strata, the experimental result are applied to compare with theoretical values for model validation .

4. Result and Discussion

Results and discussion are presented in tables including graphical representation of bacillus concentration

Table 1: Predictive values of Zinc concentration at Different Depths

Depth [M]	Predictive Values Conc. [Zinc] [Mg/L]
3	1.12
6	2.5
9	3.15
12	4.17
15	5.18
18	6.22
21	7.31
24	8.41
27	9.42
30	10.44

Table 2: Comparison of Predictive and Measured Values of zinc Concentration Different Depth

Depth [M]	predicted Values [Zinc] Conc. [Mg/L]	Measured Values[Zinc] Conc. [Mg/L]
3	1.12	0.97
6	2.5	2.73
9	3.15	3.18
12	4.17	4.22
15	5.18	5.25
18	6.22	6.33
21	7.31	7.42
24	8.41	8.57
27	9.42	9.58
30	10.44	10.51

Table 3: Predictive values of zinc concentration at Different Depth

Depth [M]	Predictive Values [Zinc] [Mg/L] Conc.
3	8.49E-05
6	8.22E-05
9	1.32E-04
12	3.45E-04
15	4.48E-04
18	5.16E-04

21	**5.88E-04**
24	**6.81E-04**
27	**7.63E-04**
30	**8.53E-04**
33	**9.32E-04**
36	**1.19E-03**

Table 4: Comparison of Predictive and Measured Values of Zinc Concentration Different Depth

Depth [M]	Predicted Values [Zinc] Conc. [Mg/L].	Measured values [Zinc] Conc. [Mg/L]
3	**8.49E-05**	**8.51E-05**
6	**8.22E-05**	**8.33E-05**
9	**1.32E-04**	**1.39E-04**
12	**3.45E-04**	**3.51E-04**
15	**4.48E-04**	**4.57E-04**
18	**5.16E-04**	**5.26E-04**
21	**5.88E-04**	**5.90E-04**
24	**6.81E-04**	**6.85E-04**
27	**7.63E-04**	**7.74E-04**
30	**8.53E-04**	**8.62E-04**
33	**9.32E-04**	**9.41E-04**
36	**1.19E-03**	**1.23E-03**

Table 4: Predictive values of Zinc concentration at Different Depth

Depth [M]	Predictive Values [Zinc] Conc. [Mg/L].
3	4.77E-03
6	9.81E-03
9	1.45E-02
12	2.22E-02
15	2.56E-02
18	3.33E-02
21	3.55E-02
24	4.33E-02
27	4.56E-02
30	5.21E-02
33	5.60E-02
36	6.32E-02

Figure 5: Comparison of Predictive and Measured Values of zinc Concentration Different Depths

Depth [M]	Predicted Values [Zinc] Conc. [Mg/L]	Measured Values [Zinc] Conc. [Mg/L].
3	4.77E-03	5.15E-03
6	9.81E-03	9.95E-03
9	1.45E-02	1.52E-02
12	2.22E-02	2.32E-02
15	2.56E-02	2.68E-02
18	3.33E-02	3.42E-02
21	3.55E-02	3.65E-02
24	4.33E-02	4.47E-02
27	4.56E-02	4.61E-02
30	5.21E-02	5.29E-02
33	5.60E-02	5.73E-02
36	6.32E-02	6.46E-02

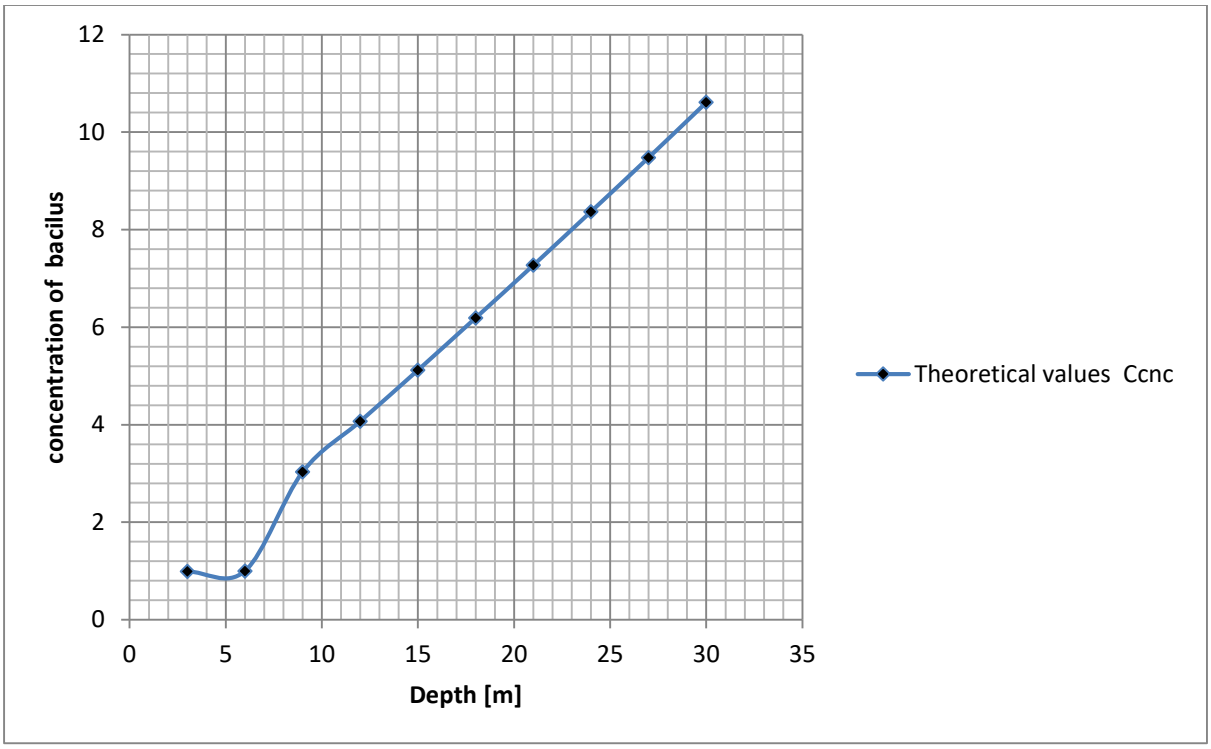

Figure 1: Theoretical values of zinc concentration at Different Depth

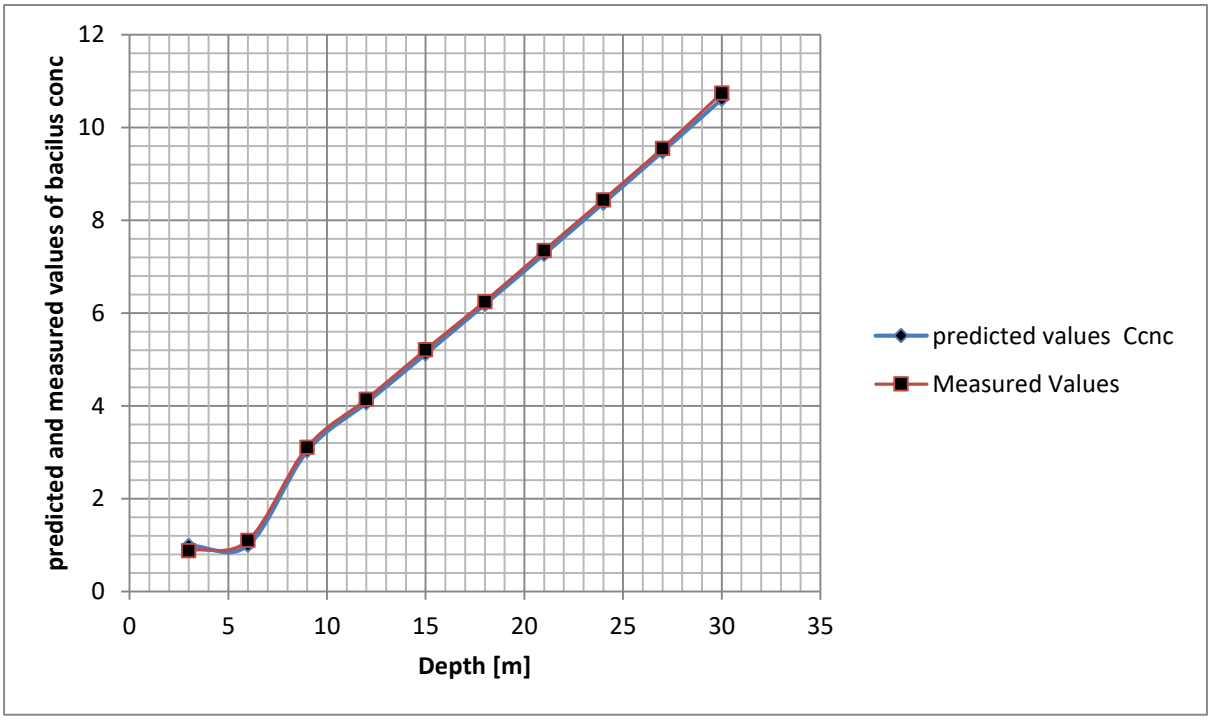

Figure 2: Comparison of Predictive and Measured Values of zinc Concentration Different Depth

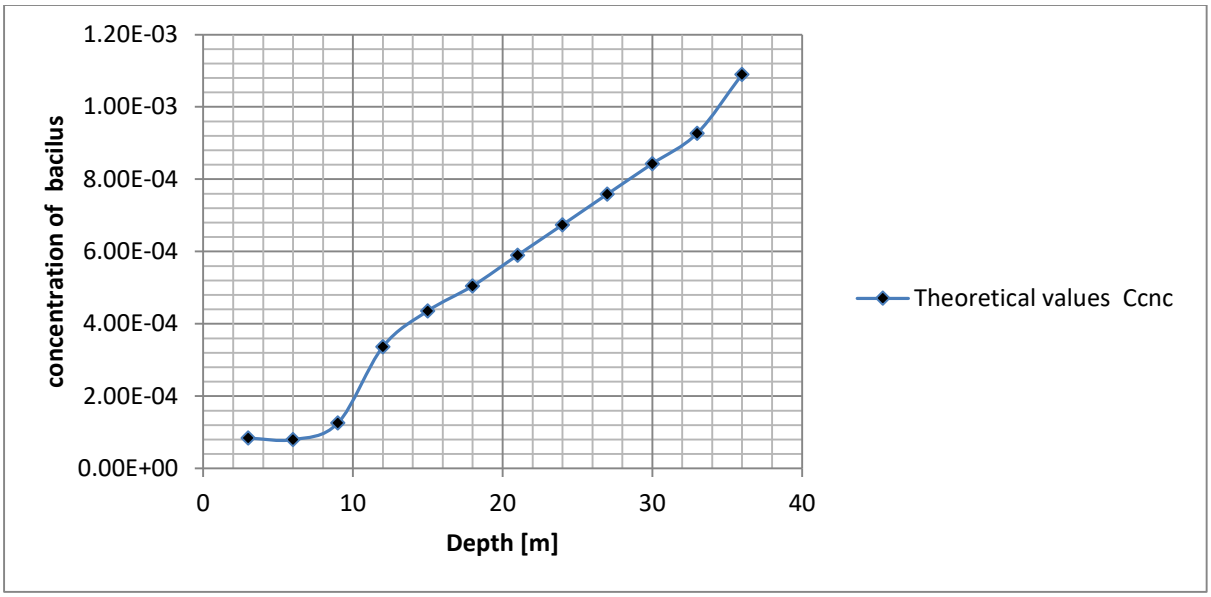

Figure 3: Predictive values of zinc concentration at Different Depth

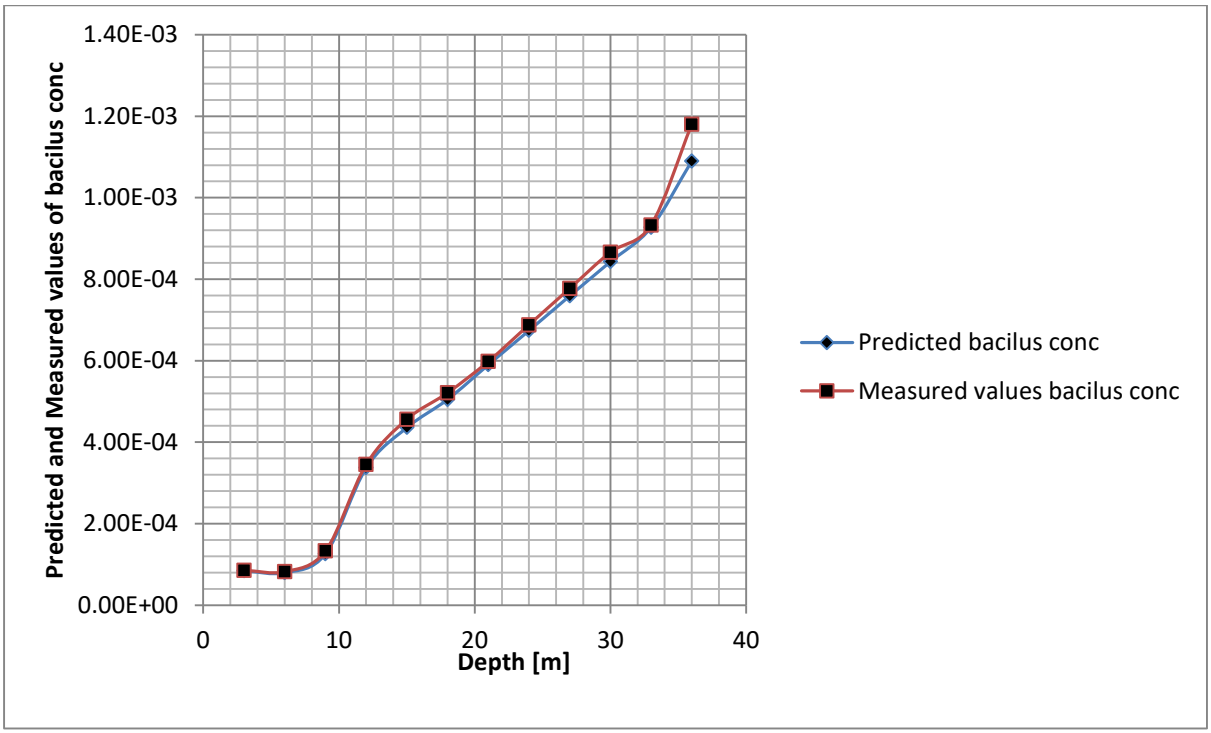

Figure 4: Comparison of Predictive and Measured Values of zinc Concentration Different Depth

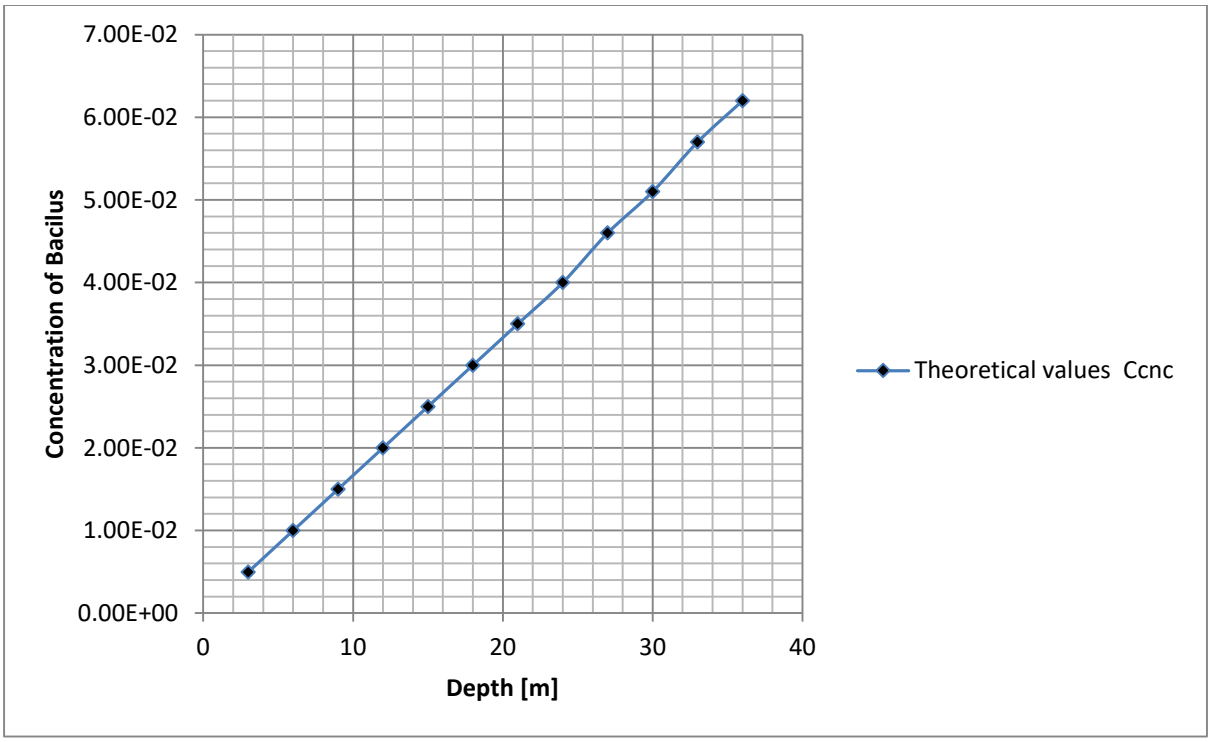

Figure 5: Predictive values of zinc concentration at Different Depth

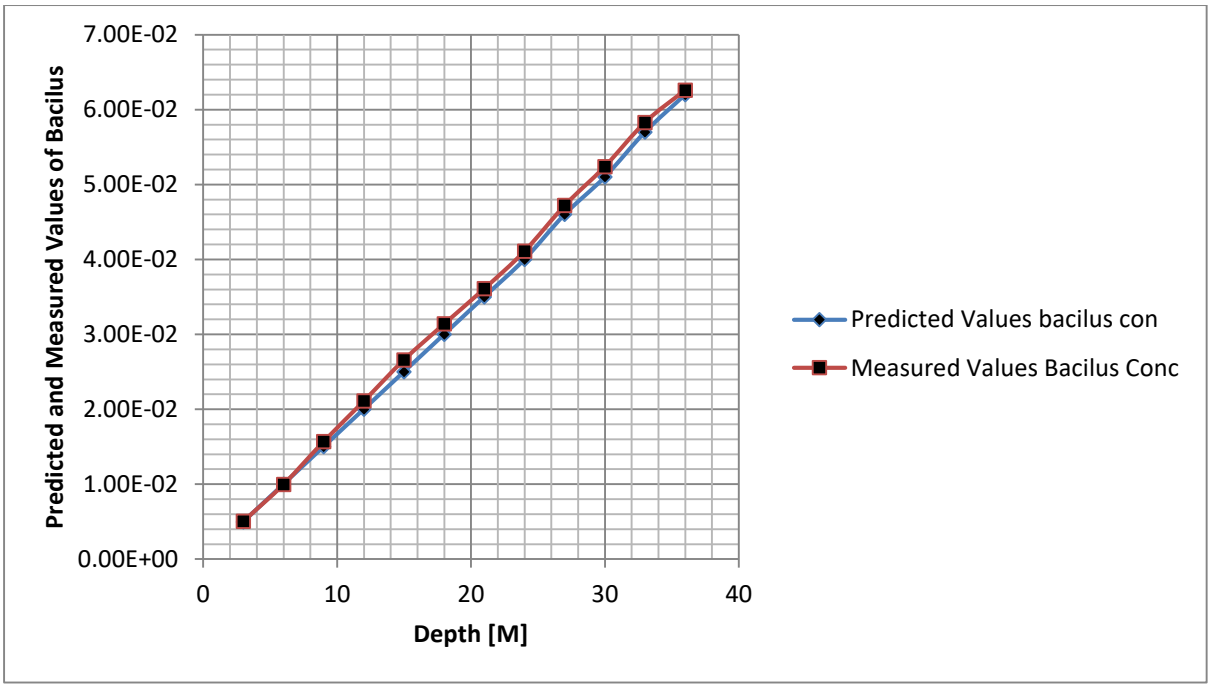

Figure 6: Comparison of Predictive and Measured Values of Zinc Concentration Different Depth

The study presented graphically shows the behaviour of zinc concentration various predominant sand gravel deposition, the study were to determine the zinc influenced by velocity rate of flow in different predominant sand gravel formation, from the graphical representation in figure one to six there is low deposition and slight fluctuation due to variation on the transition from one deposit to another, slight vacillation were observed, but the flow deposition were very low in some locations. Furthermore, other deposited area experiences higher velocity pressure in the system with the same slight fluctuation, the behaviour shows that the stratification from geological setting in the deltaic formations may developed some homogeneous higher pressure flow in those formation, this implies that high yield aquifer may found to deposit, but cannot ascertain the quality of ground water depositions in such formations, the derived solution generated theoretical values from the simulation, these values were compared with experimental results for validation, both parameters compared faviourable well thus express the authenticity of the model for the study.

4. Conclusion

The study of zinc concentration influenced by velocity of flow for sand gravel was to monitor the pressure of flow in such predominant deposition, the behaviour express the rate of stratification base on its geological setting in the study location, various flow in predominant deposited sand gravel can be applied for different purpose in soil and water engineering, monitoring of such velocity of flow influenced on zinc transport determined its rates of fluids flow in the formation, these can be applied for design of environmental systems, the study express the rate of these zinc transport pressured by linear velocity of flow at different depth between three and thirty six metres, application of mathematical modelling approach were found necessary to monitor the deposition of the fluids velocity pressured on zinc concentration at different depth in predominant sand gravel formation. Experts in soil and water engineering will definitely find use in this developed model for environmental system design.

References

[1] Cui, Y.J., Tang, A.M., Loiseau, C., Delage, P., 2008. Determining the unsaturated hydraulic conductivity of a compacted sand-bentonite mixture under constant-volume and free-swell conditions. Physics and Chemistry of the Earth, Parts A/B/C, 33 (Supplement 574 1), S462 - S471.

[2] Cui, Y.J., Tang, A.M., Qian, L.X., Ye, W.M., Chen, B., 2011. Thermal-mechanical behavior of compacted GMZ Bentonite. Soils and Foundations, Vol. 51, No. 6, 1065-1074

[3] Cui, Y.J., Loiseau, C. and Delage, P., 2002. Microstructure changes of a confined swelling soil due to suction controlled hydration. Unsaturated soils: proceedings of the Third International Conference on Unsaturated Soils, 10-13, March 2002, Recife, Brazil, 570 593-598.

[4] Juvankoski, M., 2010. Description of basic design for buffer (working report 2009-131). 612 Technical report, EURAJOKI , FINLAND

[5] Komine, H. and Yasuhara, K. and Murakami, S. 2009. Swelling characteristics of bentonites in artificial seawater. Canadian Geotechnical Journal. 46, 177-189

[6] Komine, H., 2010. Predicting hydraulic conductivity of sand bentonite mixture backfill before and after swelling deformation for underground disposal of radioactive wastes. Engineering Geology. 114, 123-134

[7] Komine, H., Watanabe, Y., 2010. The past, present and future of the geo-environment in Japan. Soils and Foundations, Vol. 50 (2010) No. 6 977-982.

[8] Martin, P.L., Barcala, J.M., and Huertas, F., 2006. Large-scale and long-term coupled 641 thermo-hydro-mechanic experiments with bentonite: the febex mock-up test. Journal of 642 Iberian Geology, 32(2), 259-282.

[9] Villar, M.V., Lloret, A., 2008. Influence of dry density and water content on the swelling of a 672 compacted bentonite. Applied Clay Science, 39(1-2), 38-49.

[10] Ye, W.M., Cui, Y.J., Qian, L.X., and Chen. B., 2009. An experimental study of the water 679 transfer thro ugh confined compacted gmz bentonite. Engineering Geology, 108(3-4), 680 169-176.

[11] Yahia-Aissa, M., Delage, P., & Cui, Y.J. 2001. Suction-water relationship in swelling clays. 676 Clay science for engineering, IS-Shizuoka International Symposium on Suction, Swelling, 677 Permeability and Structure of Clays, 65-68, Adachi & Fukue eds, Balkema

[12] Pusch, R., 1979, Highly compacted sodium bentonite for isolating rock-deposited 645 radioactive
646 waste products. Nucl. Technol.;(United States), 45(2).

[13] Yong, R.N., Boonsinsuk, P., and Wong, G., 1986. Formulation of backfill material for a 682 nuclear fuel waste disposal vault. Canadian Geotechnical Journal, 23(2), 216-228.

Qiong Wang1, Anh Minh Tang Yu-Jun Cui1, Pierre Delage1, Jean-Dominique Barnichon Wei-Min Ye3